Harmonic radiation emission from periodic lattices irradiated by short-pulse elliptically polarized laser light

R. Ondarza-Rovira
Instituto Nacional de Investigaciones Nucleares, Apartado Postal 18-1027, México 11801, Distrito Federal, Mexico

T. J. M. Boyd
Physics Department, University of Essex, Wivenhoe Park, Colchester CO4 3SQ, United Kingdom

(Received 31 January 2001; revised manuscript received 14 May 2001; published 21 September 2001)

Radiated emission at high-order harmonic numbers is observed from thin crystalline layers irradiated by short femtosecond elliptically polarized laser light. The applied external radiation field drives the free electrons in the material to large oscillation amplitudes and harmonics are generated by the electronic response to the periodic lattice potential. A model was modified by introducing a more general expression for the lattice force that by sharpening or by smoothing the potential in turn allows the strength of the electronic perturbation to be varied. The electron motion is computed numerically by solving the electromagnetic force equation and by regarding the lattice potential as a perturbative source. For linearly polarized laser light the radiation spectra are characterized by emission lines forming a flat plateau in the region of low harmonic orders with a sharp cutoff for higher numbers. For circular polarization strong emission is found for two harmonic numbers, the first in the low-harmonic region and the second around the cutoff. By solving analytically the electron motion in an elliptically polarized laser field, an exact expression for the electron displacement in all three spatial directions is found. The amplitude of the oscillations sets the analytic form for calculating the peak harmonic numbers emitted from the laser-lattice interaction. The radiation effect studied here, if detected, might hold some potential as a diagnostic and could be used, in principle, as a method for determining the lattice parameter in crystalline structures.

DOI: 10.1103/PhysRevE.64.046604 PACS number(s): 42.65.Ky, 52.25.Os, 41.60.−m

I. INTRODUCTION

Recent theoretical and computational work on the irradiation of thin solid layers by short-pulse moderately intense lasers has drawn attention to the high-order harmonic emission that can be generated [1,2]. The model proposed by Hüller and Meyer-ter-Vehn [1] to explain harmonic generation from the interaction of an electromagnetic laser wave with thin film targets describes the mechanism as one in which the free electrons inside the material are driven by the applied field to large amplitude excursions. Perturbations in the electron motion due to the ion cores give rise to harmonic emission. Results reported in [1] predict that ionized electrons, under both the action of a linearly polarized laser field and a periodic ion potential, radiate a spectrum of harmonics featured by a flat plateau over the region of low harmonic numbers and a sudden cutoff around the maximum harmonic number emitted. It was shown that the maximum harmonic order emitted depends on the lattice spacing and on the laser wavelength and input energy. The model described in [1] was modified in [2] by proposing a more general expression for the lattice potential that by sharpening or by smoothing the potential in turn allows the strength of the perturbation to be varied. The effects of pulse shaping on the radiation emission were also considered. In particular, for Gaussian pulses, the strongest emission was found to be emitted by lower harmonic numbers and a cutoff was still observed. The mechanism of harmonic generation studied here is distinct from the emission observed when highly intense laser light illuminates a solid surface or a dense plasma. In early experiments carried on by Carman *et al.* [3], the emission was attributed to nonlinear resonant absorption with the plasma wave coupling to the radiation field in the steep density gradient profile and generating harmonics. From those experiments a sharp cutoff at high harmonic numbers was found. This characteristic emission was erroneously interpreted as the maximum harmonic for which the upper density shelf went underdense. Low temporal and spatial resolution miscalculations led to an incorrect interpretation in Carman's proposed model.

Recent advances in laser technology have allowed development of devices capable of delivering high intensities ($\geqslant 10^{18}\,\mathrm{W/cm^2}$) and ultrashort pulses ($\sim$10 fs) in plasmas. In such experiments no cutoff features in the emission spectra have been observed, as was predicted in numerical simulations performed by Gibbon [4].

Presumably, when external electromagnetic radiation is incident on steep density profile dense plasmas, density fluctuations on the plasma surface are induced, constituting sources for harmonic generation [5–7].

The radiation mechanism considered in this work presents features in common with the Smith-Purcell (SP) effect [8–10], an effect independently found by Salisbury [11], in which radiation arises from the passage of highly energetic electrons ($\geqslant$50 keV) through a periodical array of grooves in the surface of a grating. In the SP effect coherent band radiation is emitted from the radio to ultraviolet spectral regions with frequency $\omega = \mathbf{k}_g \cdot \mathbf{v}(1-\beta\cos\theta)^{-1}$, where $\mathbf{k}_g$ is the grating periodicity, $\mathbf{v}$ denotes the velocity of a beam electron, $\beta = v/c$, and θ is the angle between the beam direction and the source-observer axis.

The radiation in a periodic medium is composed of emission at different harmonic orders. The condition for radiation, the resonance condition, can be derived on the basis of conservation laws for the momentum and the energy. Using this idea, it will be shown that the crystal lattice might be regarded as a periodic diffractive grating responsible of emission when charged particles, driven by an external electromagnetic field, traverse arrays of ion cores inside the solid lattice. The remainder of this work is organized as follows. In Sec. II we review the model for harmonic emission from periodic lattice arrays and Sec. III outlines the numerical procedure for computing the electron dynamics for an elliptically polarized light field. In Sec. IV we account for the exact analytical solution of the dynamics of electrons driven by an electromagnetic field with elliptic polarization. Section V examines the resonance condition for radiation. Lastly, a discussion of the results presented is addressed in Sec. VI.

II. HARMONIC EMISSION FROM DRIVEN ELECTRONS IN A PERIODIC LATTICE: LINEAR POLARIZATION

In this section we briefly review aspects of the radiation phenomena from the electron quiver motion in a crystalline array, as first treated in Refs. [1] and [2]. The transverse quiver momentum of an electron embedded in a light field is given by $\mathbf{p}=m_0 c\mathbf{a}_0$, where $\mathbf{a}_0=e\mathbf{A}_0/m_0c^2$ is the unitless normalized vector potential of the incident radiation field. Here e, c, m_0, and $\mathbf{A}_0$ denote the electron charge, the speed of light in vacuum, the electron rest mass, and the vector potential, respectively. Denoting the magnitude of the normalized vector potential as

$$a_0 \simeq 8.544\times 10^{-10} I_L^{1/2}\ (\mathrm{W/cm^2})\times \lambda_L\ (\mu\mathrm{m}),$$

where λ_L is the laser wavelength in micrometers and I_L is the field intensity, we can express the velocity of oscillation as $v_{\mathrm{osc}}=ca_0/\gamma_\perp$, where $\gamma_\perp \simeq (1+a_0^2)^{1/2}$ is the relativistic factor associated with the transverse electron motion. Although the model proposed is valid only for low-intense field intensities, we have made use—for completeness—of a relativistic formulation. Thus, the analytic expressions throughout this work must therefore be considered classical, with $\gamma \sim 1$.

At high laser intensities the crystalline structure might be affected by the action of the radiation field. Distortions to the lattice configuration can produce alterations in the harmonicity of the electron motion through the ion cores. Nevertheless, the lattice structure can preserve its initial configuration when ultrashort and low-intense laser pulses are applied. It has been shown from a number of experimental works that ultrashort femtosecond laser pulses at intensities lower than $10^{11}\,\mathrm{W/cm^2}$ can be applied without impinging important damage on a crystalline structure [12,13]. Laser-induced disorders of material surfaces for pulses of duration 100 fs at peak intensities of tenths of $\mathrm{J/cm^2}$ have been observed [14,15], and where a loss of cubic order was found 150 fs after the pulse. Taking the above into consideration, for the time scale and laser power, we have used in our simulations CO_2 ($\lambda_L=10.6\,\mu$m) laser light with pulse duration of only a few femtoseconds ($\sim$40 fs), allowing quiver excursions $\delta=(\lambda_L/2\pi)a_0$ greater than the lattice spacing l_c. For instance, for $I_L=5\times 10^{10}\,\mathrm{W/cm^2}$ ($a_0\sim 2.025\times 10^{-3}$) the lattice electrons execute oscillation amplitudes of $\delta/l_c\sim 9$, with l_c taken as 4 Å.

The classical equation of motion for free electrons in a solid material under the influence of both a plane monochromatic linearly polarized electromagnetic wave and a lattice potential $\phi(\mathbf{r})$ can be expressed in the form

$$m_0\ddot{\mathbf{r}}(t) = -e\mathbf{E}_L \sin(\omega_L t - \mathbf{k}_L\cdot\mathbf{r}) + e\boldsymbol{\nabla}\phi(\mathbf{r}). \tag{1}$$

Essentially, the electron trajectories consist of harmonic oscillations $\mathbf{r}(t)=\mathbf{r}_0+\mathbf{r}_1(t)+\mathbf{r}_2(t)$, around centers $\mathbf{r}_0$, where $\mathbf{r}_1(t)=\boldsymbol{\delta}\sin(\omega_L t-\mathbf{k}_L\cdot\mathbf{r}_0)$ is the quiver electron motion with amplitude $\boldsymbol{\delta}=e\mathbf{E}_L/m_0\omega_L^2$ and $\mathbf{r}_2(t)$ corresponds to small deviations produced by the perturbation of the lattice force. With the aim of representing the periodic lattice force acting on electrons as they make excursions through the crystalline array we considered a potential $\phi(\mathbf{r})$ of the form

$$\phi(\mathbf{r}) = \sum_c\ \phi_c \sinh[A\sin(\mathbf{k}_c\cdot\mathbf{r})], \tag{2}$$

where $\mathbf{k}_c=k_c\hat{\mathbf{e}}_c$ corresponds to the reciprocal lattice vectors and the strength amplitude ϕ_c is of the order of one volt for typical metals [16]. The factor A in the last expression can be incorporated into the model in order to include variations in the lattice potential. The lattice potential considered in Eq. (2) can be reduced to the conventionally used sinusoidal potential and so applied in Ref. [1].

Following Hüller and Meyer-ter-Vehn's model and incorporating a more general expression for the lattice potential, as considered above, the lattice force gives rise to a perturbed motion described by

$$m_0\ddot{\mathbf{r}}_2 \sim -\sum_c\ e\mathbf{A}\phi_c\mathbf{k}_c\cos(\mathbf{k}_c\cdot\mathbf{r})\cosh[A\sin(\mathbf{k}_c\cdot\mathbf{r})].$$

Harmonics are generated due to the lattice force $m_0\ddot{\mathbf{r}}_2(t')$, evaluated at the retarded time $t'=t-\boldsymbol{\Omega}\cdot(\mathbf{R}_{\mathrm{obs}}-\mathbf{r})/c$, where $\boldsymbol{\Omega}$ is a unit vector from the particle to the observer and $\mathbf{R}_{\mathrm{obs}}$ is the vector from the origin to the observation point. In what follows, the prime has been dropped for convenience. Using Jacobi expansions for the arguments, the acceleration can be expressed as

$$\ddot{\mathbf{r}}_2 \sim -\sum_c\ \frac{e}{m_0}\phi_c\mathbf{k}_c A\sum_m\ \epsilon_m J_m(Z)\cos\alpha(t)\cos\beta \times\cosh\left(A\sum_m\ \epsilon_m J_m(Z)\cos\alpha(t)\sin\beta\right), \tag{3}$$

where

$$\alpha(t)=\tfrac{1}{2}m\pi-\omega_L t+b,$$

$$\beta=\tfrac{1}{2}m\pi+\mathbf{k}_c\cdot\mathbf{r}_0,$$

$$Z=\mathbf{k}_c\cdot\boldsymbol{\delta},$$

$$b=k_L\boldsymbol{\Omega}\cdot\mathbf{r}-\mathbf{k}_L\cdot\mathbf{r}_0-\frac{\omega_L}{c}\boldsymbol{\Omega}\cdot\mathbf{R}_{\rm obs}.$$

The power radiated by single electrons per unit solid angle in the direction $\boldsymbol{\Omega}$ is given by [17]

$$\frac{dP(t)}{d\Omega}=\frac{c}{4\pi}|R\mathbf{E}_{\rm rad}(t,\Omega)|^2,$$

where

$$\mathbf{E}_{\rm rad}(t,\Omega)=-\frac{e}{c^2}\boldsymbol{\Omega}\times[\boldsymbol{\Omega}\times\ddot{\mathbf{r}}(t')]/R,$$

and $\mathbf{R}=|\mathbf{R}_{\rm obs}-\mathbf{r}|$.

The spectral components are then obtained by evaluating and Fourier analyzing the acceleration field. The emission calculated by means of this procedure is in accordance with that obtained by numerically integrating the electron force equation, a step we follow in the next section.

In order to have insight into the maximum harmonic number that can be generated from the action of the lattice force on the electron motion we follow a procedure that involves conservation of energy and momentum.

The radiation spectrum produced when a charged particle moves in the vicinity of a periodic structure can be explained from conservation laws. Radiation arises only if resonance conditions are fulfilled. To explain the last statement, let us assume that the medium changes its properties periodically along a certain direction. If we consider a particle traveling through a medium with velocity v emitting quanta of energy $\hbar\omega$ and momentum $\hbar\omega/c$, the conservation laws for the longitudinal momentum and the energy can be written in general form as

$$\frac{\mathbf{v}\cdot\delta\mathbf{p}}{v}-\frac{\hbar\omega}{c}\cos\theta'=\frac{2\pi}{l}n,$$

$$\delta E-\hbar\omega=0,$$

where θ' is the angle between the direction of a quantum emitted and the velocity $\mathbf{v}$. The changes in energy and momentum of the particle are denoted by δE and $\delta\mathbf{p}$, respectively, n is an arbitrary integer, and l the periodicity of the medium. Since $\delta E=\mathbf{v}\cdot\delta\mathbf{p}$ for small changes of the energy of the particle, the condition for radiation from the conservation laws reads

$$\frac{\omega_{\rm eff}}{v}\equiv\frac{\omega}{v}\left(1-\frac{v}{c}\cos\theta'\right)=\frac{2\pi m}{l}.$$

For the finite plane-wave–solid interaction, the spectrum forms a plateau in the region of low harmonic orders with a cutoff near the peak intensity. The location of the cutoff can then be derived from the resonance condition $n_{\rm max}\omega_L\sim k_c v_{\rm osc}$, which yields

$$n_{\rm max}\simeq\left(\frac{\lambda_L}{l_c}\right)\frac{a_0}{\gamma_\perp},\tag{4}$$

where l_c is the lattice spacing.

The overall strength of the spectrum is determined by the electron distribution. From the analysis of the phase factors involved in the expression for the acceleration field it can be shown that correlations between electrons are important [1], in the sense that for cases in which the electrons are correlated the radiation emitted will be enhanced and at the same time will produce only harmonics of odd order. For disordered electron systems, the emission is found to be less intense and harmonics of any order are permitted. The former case—which represents a more realistic electron behavior—would correspond to oscillation centers that cluster at the sites of the ions or at interstitial locations.

III. NUMERICAL COMPUTATION OF THE RADIATION EMISSION

In order to study the dynamics of electrons in the applied radiation field a single-particle force equation for an elliptically polarized electromagnetic plane wave with the lattice potential term as an external source was solved. The electron dynamics was examined by means of the numerical solution of the force equation

$$\frac{d\mathbf{p}}{dt}=-e\mathbf{E}-\frac{e}{c}\mathbf{v}\times\mathbf{B}+e\boldsymbol{\nabla}\phi.\tag{5}$$

We consider the lattice potential as that given by $\phi(\mathbf{r})$ in expression (2). Variations of the lattice potential and its role in harmonic generation will be considered in a future publication.

For a monochromatic plane wave of arbitrary polarization, with propagation vector along the x direction, the vector potential can be expressed as

$$\mathbf{A}(\mathbf{r},t)=a(\eta)(0,(1-\delta^2)^{1/2}\sin\eta,\delta\cos\eta),\tag{6}$$

where $a(\eta)$ is a shape factor. Here, $\eta=\omega_L(t-x/c)$ is the Lorentz invariant phase. The propagation is taken in the direction of the Poynting vector. The parameter δ $(0\leqslant\delta\leqslant1)$ characterizes the degree of elliptic polarization. Linear polarization corresponds to $\delta=0,\pm1$ and circular polarization to $\delta=\pm1/\sqrt{2}$.

Pulse shape effects for the case of a linearly polarized wave incident on a lattice array were considered in Ref. [2].

Using the expression for the electromagnetic potential, as well as the gauge field equations, the components of the force equation take the form

$$\dot{v}_x=\frac{a_0\omega_L}{\gamma}\left(1-\frac{v_x}{c}\right)[v_z\delta\sin\eta-v_y(1-\delta^2)^{1/2}\cos\eta]+F_p^x,\tag{7}$$

$$\dot{v}_y = -\frac{a_0\omega_L c}{\gamma}\left\{\left(1-\frac{v_x}{c}\right)\left(1-\frac{v_y^2}{c^2}\right)(1-\delta^2)^{1/2}\cos\eta + \frac{v_y v_z}{c^2}\delta\sin\eta\right\} + F_p^y, \tag{8}$$

$$\dot{v}_z = \frac{a_0\omega_L c}{\gamma}\left\{\left(1-\frac{v_x}{c}-\frac{v_z^2}{c^2}\right)\delta\sin\eta + \frac{v_y v_z}{c^2}(1-\delta^2)^{1/2}\cos\eta\right\} + F_p^z, \tag{9}$$

$$\dot{\gamma} = \frac{a_0\omega_L}{c}(v_z\delta\sin\eta - v_y(1-\delta^2)^{1/2}\cos\eta) + \frac{e}{m_0c^2}(\mathbf{v}\cdot\boldsymbol{\nabla}\phi). \tag{10}$$

Here, γ is the relativistic factor given by $\gamma=(1-\beta^2)^{-1/2}$ and $\beta=v/c$. F_p^i $(i=x,y,z)$ stands for the components of the lattice force given by

$$F_p^x = -\frac{e}{m_0\gamma}\left\{\left(1-\frac{v_x^2}{c^2}\right)(\nabla\phi)_x - \frac{v_x v_y}{c^2}(\nabla\phi)_y\right\}, \tag{11}$$

$$F_p^y = -\frac{e}{m_0\gamma}\left\{\left(1-\frac{v_y^2}{c^2}\right)(\nabla\phi)_y - \frac{v_y v_x}{c^2}(\nabla\phi)_x\right\}, \tag{12}$$

$$F_p^z = \frac{e v_z}{m_0c^2\gamma}\{v_x(\nabla\phi)_x + v_y(\nabla\phi)_y\}. \tag{13}$$

With the aim of verifying the numerical integration of the force equations during the pulse duration we have applied the conservation of energy which can be expressed in terms of the electron velocities in the form

$$\gamma^3\sum_i v_i\dot{v}_i = \frac{e}{m_0}\sum_i v_i(E_i+(\nabla\phi)_i).$$

The numerical integration performed here was carried out using atomic units, in which $e=m_0=\hbar=1$ and $c=137.07$. In this metric the most used units are given as 1 g$=1.098\times10^{27}$ a.u., 1 cm/sec$=4.572\times10^{-9}$ a.u., 1 sec $=4.132\times10^{16}$ a.u., 1 cm$=1.889\times10^{8}$ a.u., 1 V/cm$=1.945\times10^{-10}$ a.u., and 1 W$=5.554$ a.u.

The numerical procedure outlined here reproduces the emission spectrum with the plateau and the cutoff obtained by Hüller and Meyer-ter-Vehn [1] for a thin solid layer illuminated by a linearly polarized laser pulse. The cutoffs were found at the predicted values $n_{\max}$, as given by Eq. (4). Figure 1 shows the radiation spectrum for a laser intensity of $I_L=5\times10^9$ W/cm^2. The lattice period is taken as $l_c=4$ Å. For this case, the electrons traverse through seven lattice sites in an optical cycle and the spectrum forms a well-defined plateau with a cutoff around $m=16$, as predicted by expression (4). Here, m stands for the harmonics $\omega_m=m\omega_L$. The peak intensity is near the cutoff value. The spectrum is normalized by a factor $f_n=4.74\times10^{-14}$, and does not show emission at the fundamental frequency ω_L.

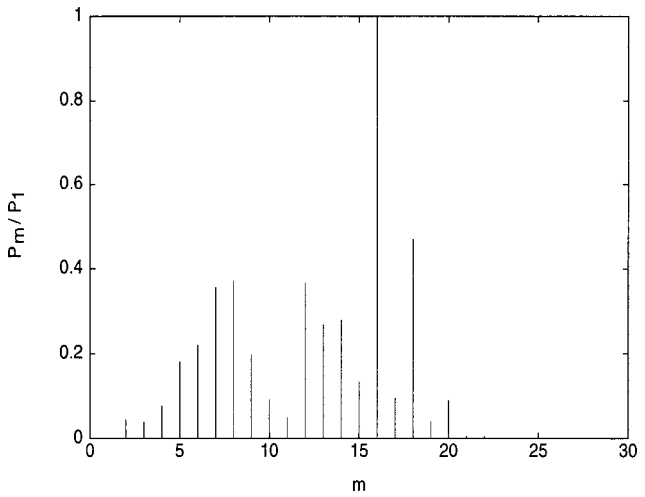

FIG. 1. Radiation spectrum for linear polarization. $I_L=5\times10^9$ W/cm^2, $\lambda_L=10.6\,\mu$m, $l_c=4$ Å, and $m=\omega_m/\omega_L$.

For a circularly polarized laser pulse interacting with a lattice array, i.e., for the case in which $\delta=1/\sqrt{2}$ in Eq. (6), we have performed single-particle simulations for the case $I_L=5\times10^9$ W/cm^2 and $\lambda_L=10.6\,\mu$m without the influence of the lattice potential. In Fig. 2 the electron trajectory in the y-z plane is shown.

Figures 3–5 show the electron displacement in all three spatial coordinates. The electron dynamics, as we will see in the next section, are in accordance with the analytical solutions obtained for the equation of motion in an electromagnetic field with elliptic polarization.

The corresponding radiated emission once the lattice potential is considered is shown in Fig. 6. Here, $f_n=1.9\times10^{-13}$. An unexpected characteristic feature observed in the emission spectra is the appearance of two strong peaks, at $m=8$ and at $m=31$, rather than a single peak as found in the linearly polarized case. As will be demonstrated in the following section both emission peaks originate from a coupling effect between those different electromagnetic modes

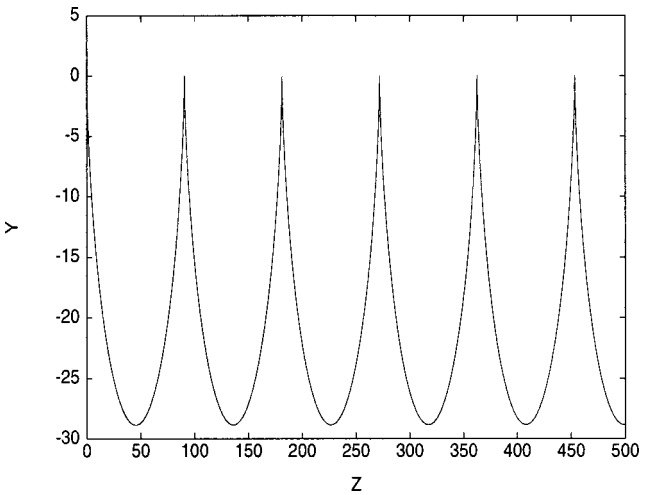

FIG. 2. Electron trajectory in the y-z plane for circular polarization. $I_L=5\times10^9$ W/cm^2 and $\lambda_L=10.6\,\mu$m; variables are expressed in atomic units.

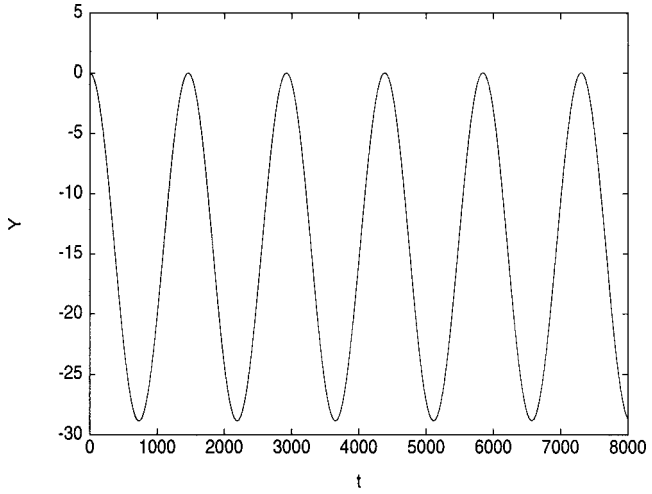

FIG. 3. Electron motion in the *y* direction for circular polarization. Parameters as in Fig. 2.

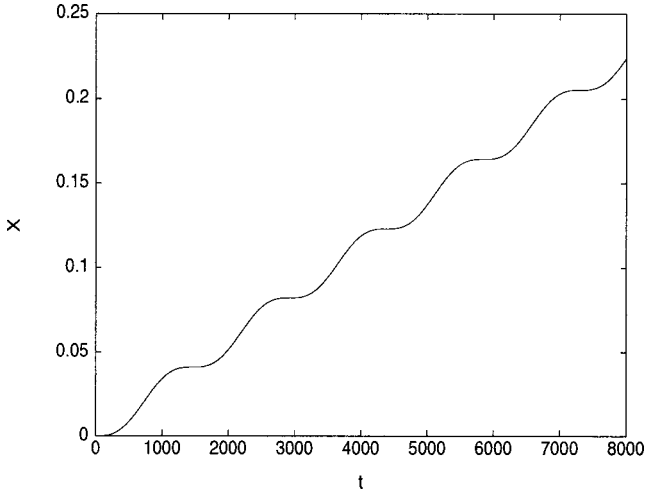

FIG. 5. Electron motion in the *x* direction for circular polarization. Parameters as in Fig. 2.

excited from the resonance conditions, corresponding to all three spatial directions. In other words, the electrons execute main excursions along a bidimensional array in the plane y-z, with a drift along the direction of propagation of the wave, and from each of those excursions radiation is emitted. As for the linearly polarized case the electrons perform harmonic motions along lines of equidistant ion cores.

In Fig. 7 the emission for the case of a laser intensity $I_L = 5\times10^{10}\,\mathrm{W/cm^2}$ is plotted, with $f_n = 2.9\times10^{-12}$. For this case, two strong peaks around $m=25$ and 100 are emitted. As we will see, both numbers are in accordance with the analytical prediction that will be presented in Sec. IV.

IV. ANALYTICAL SOLUTION OF THE EQUATIONS OF MOTION

With the aim of obtaining an analytical expression for the dynamics of charged particles moving in an external elliptically polarized laser field we solve the equations of motion for free electrons without the action of other external sources. From the electron displacement and the size of the excursion in all three spatial directions we will derive the resonance condition for those harmonic numbers that correspond to the peak intensities in the emitted spectra.

From the equation of motion we have

$$\frac{d}{dt}(\gamma v_y) = -a_0 c(1-\delta^2)^{1/2}\dot{\eta}\cos\eta,$$
$$\frac{d}{dt}(\gamma v_z) = a_0 c\,\delta\dot{\eta}\sin\eta, \tag{14}$$

where $\dot{\eta}=\omega_L(1-v_x/c)$. On the other hand, we have that

$$\frac{d}{dt}(\gamma v_x) = \frac{d}{dt}(\gamma c),$$

from which we get

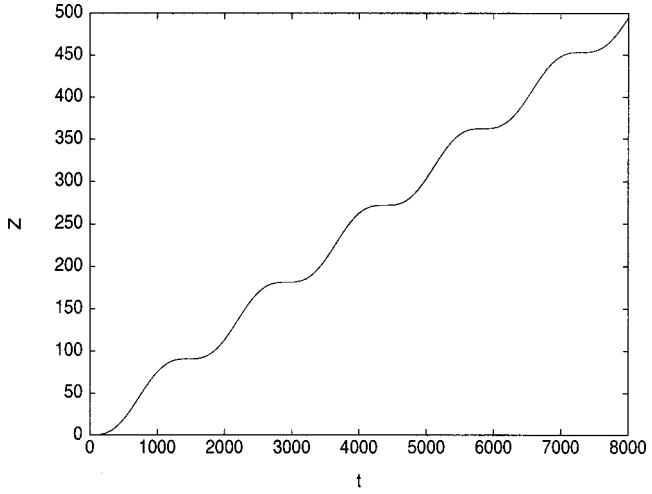

FIG. 4. Electron motion in the *z* direction for circular polarization. Parameters as in Fig. 2.

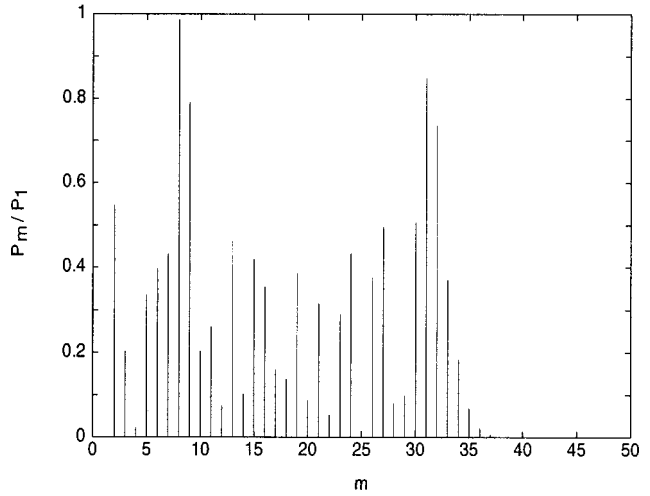

FIG. 6. Radiation spectrum for circular polarization. Parameters as in Fig. 2, $l_c = 4$ Å and $m=\omega_m/\omega_L$.

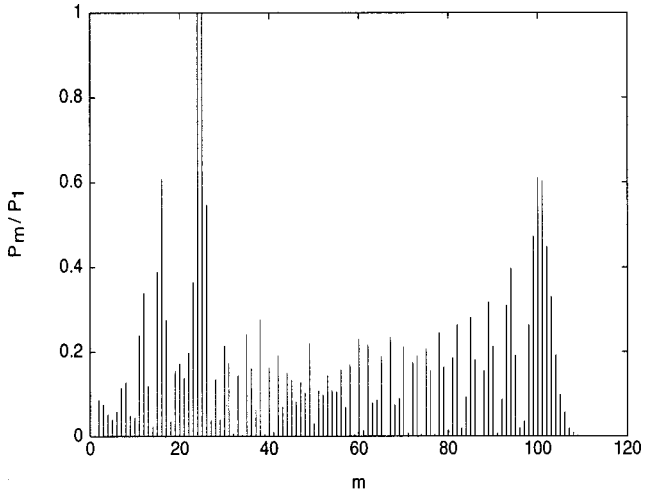

FIG. 7. Radiation spectrum for circular polarization. $I_L=5\times10^{10}\,\mathrm{W/cm^2}$, $\lambda_L=10.6\,\mu\mathrm{m}$, $l_c=4$ Å, and $m=\omega_m/\omega_L$.

$$\gamma=\left(1-\frac{\dot{x}}{c}\right)^{-1}=\frac{p_x+m_0c}{m_0c}. \tag{15}$$

Using the equation for the energy $E=m_0\gamma c^2=p^2c^2+m_0^2c^4$, the expression for γ and Eqs. (14) we can obtain the momenta of the particle.

Expressing the velocities in the form $v_i=(di/d\eta)\dot{\eta}$, $i=x,y,z$, and upon integration we have that the coordinates, for the case when $\delta=1/\sqrt{2}$, are given by

$$x=\frac{1}{2}\frac{a_0^2}{k}(\eta-\sin\eta),$$

$$y=-\frac{1}{\sqrt{2}}\frac{a_0}{k}(1-\cos\eta), \tag{16}$$

$$z=\frac{1}{\sqrt{2}}\frac{a_0}{k}(\eta-\sin\eta).$$

The last equations describe the trajectories for electrons driven by a circularly polarized laser field and are in agreement with their numerical counterpart shown in Figs. 3–5. The trajectory for the y component is essentially described by a sinusoidal function with amplitude $\delta_y=\lambda_L a_0/2\sqrt{2}\pi$, and quiver velocity given by $v_{qy}=2a_0c/\sqrt{2}(2+a_0^2)$. Figures 4 and 5 show that the particles drift along the x and z position coordinates, with velocities $v_{dx}=a_0^2c/(2+a_0^2)$ and $v_{dz}=\sqrt{2}a_0c/(2+a_0^2)$, respectively, as given from Eqs. (16).

V. RESONANCE CONDITION FOR RADIATION

We have seen in Sec. II that the location of the cutoff is derived from a resonance condition obtained from the conservation laws of energy and momentum. In a similar way we can locate the cutoffs in the emission spectra by using the expression for the amplitudes of the excursions for all three spatial directions. Thus, the cut-off emission corresponding to a maximum displacement in a given direction is expressed as

$$n_{\max,i}=\frac{2\pi}{l_c}\delta_i;\quad i=x,y,z, \tag{17}$$

where l_c is the lattice spacing and δ_i is the amplitude of the electron excursion for a particular coordinate. From the linear part of Eqs. (16) the amplitude of the excursions can be obtained by taking $\eta=\pi/2$, which corresponds to the value of the phase η for maximum amplitude in the electron quiver motion in the y direction, and given by

$$\delta_x=\frac{\lambda_L}{8}a_0^2,$$

$$\delta_y=\frac{\lambda_L}{2\sqrt{2}\pi}a_0,$$

$$\delta_z=\frac{\lambda_L}{4\sqrt{2}}a_0.$$

Since δ_x is an order of magnitude smaller in a_0 than the displacement in the other two directions, we have that two main modes will contribute to the emission peaks.

Coupling δ_z and δ_y in Eq. (17) we have that the emission peaks will be radiated at the harmonic numbers

$$n_{\max_+}=\left(\frac{\lambda_L}{l_c}\right)\frac{a_0}{2\sqrt{2}}(\pi+2),$$

$$n_{\max_-}=\left(\frac{\lambda_L}{l_c}\right)\frac{a_0}{2\sqrt{2}}(\pi-2). \tag{18}$$

For instance, for $I_L=5\times10^9\,\mathrm{W/cm^2}$ ($a_0\sim6.4\times10^{-4}$), $n_{\max_+}=31$, and $n_{\max_-}=8$ as obtained from the numerical computation of the dynamic equations and shown in Fig. 6. For an intensity of $5\times10^{10}\,\mathrm{W/cm^2}$ ($a_0\sim2.025\times10^{-3}$), $n_{\max_+}=100$, and $n_{\max_-}=25$ as shown in Fig. 7. The small contribution effect to the coupling from δ_x would be given by $(\pi/4)(\lambda_L/l_c)a_0^2$ with negligible values 0.0085 and 0.085 for the intensities 5×10^9 and $5\times10^{10}\,\mathrm{W/cm^2}$, respectively.

VI. CONCLUSIONS

Harmonic radiation emission from electrons driven by a short femtosecond elliptically polarized laser field and under the influence of a periodic lattice potential was obtained.

For linearly polarized laser light incident on a periodic ion array, the emission spectra were found to be characterized by harmonic numbers forming a plateau with a sudden cutoff. In the case of elliptic polarization the numerical emission spectra contain two strong emission peaks, attributable, as derived from the theory presented here, to the maximum excursion amplitude of the motion in the two directions of the plane normal to the direction of propagation of the laser light. It is found that coupling effects between the modes that

correspond to those excursion amplitudes are responsible for strong harmonic emission at two main peaks in the spectra. The contribution to the emission from the motion in the direction of propagation of the wave proved to be weaker than that mode produced by the other two directions, at least an order of magnitude in the normalized vector potential. We recall that for higher laser input energies disintegration of the lattice structure could take place, invalidating the approach presented here. The motion of free electrons embedded in an elliptically polarized laser field was solved analytically in closed form. From the analytical procedure employed in this work we derived the equations for the coordinates and calculated the magnitude of the electron excursion in all three spatial directions. From those calculations we arrived, through the condition of resonance, at the analytic expressions (18) that give the location of two maxima that correspond to the emission peaks in the spectra and whose harmonic numbers are in accordance with those obtained from numerical computations.

ACKNOWLEDGMENTS

One of the authors (R.O.-R.) is grateful to T.J. Ayhllon for encouraging support during the preparation of this work and acknowledges financial support from Consejo Nacional de Ciencia y Tecnología (CONACyT) under Contract No. 33251-E.

[1] S. Hüller and J. Meyer-ter-Vehn, Phys. Rev. A **48**, 3906 (1993).
[2] R. Ondarza-Rovira, Rev. Mex. Fis. **44**, 55 (1998).
[3] R. L. Carman, C. K. Rhodes, and R. F. Benjamin, Phys. Rev. A **24**, 2649 (1981).
[4] P. Gibbon, Phys. Rev. Lett. **76**, 50 (1996).
[5] R. Ondarza-Rovira and T. J. M. Boyd, Phys. Plasmas **7**, 1520 (2000).
[6] T. J. M. Boyd and R. Ondarza-Rovira, Phys. Rev. Lett. **85**, 1440 (2000).
[7] R. Lichters, J. Meyer-ter-Vehn, and A. Pukhov, Phys. Plasmas **3**, 3425 (1996).
[8] S. J. Smith and E. M. Purcell, Phys. Rev. **92**, 1069 (1953).
[9] M. J. Moran, Phys. Rev. Lett. **69**, 2523 (1992).
[10] G. Doucas, J. H. Mulvey, M. Omori, J. Walsh, and M. F. Kimmitt, Phys. Rev. Lett. **69**, 1761 (1992).
[11] W. Salisbury, U.S. Patent No. 2634372 (1953).
[12] P. L. Silvestrelli, A. Alavi, M. Parrinello, and D. Frenkel, Phys. Rev. Lett. **77**, 3149 (1996).
[13] K. Sokolowski-Tinten, J. Solis, J. Bialkowski, J. Siegel, C. N. Alfonso, and D. von der Linde, Phys. Rev. Lett. **81**, 3679 (1998).
[14] H. W. K. Tom, G. D. Aumiller, and C. H. Brito-Cruz, Phys. Rev. Lett. **60**, 1438 (1988).
[15] P. Saeta, J.-K. Wang, Y. Siegal, N. Bloembergen, and E. Mazur, Phys. Rev. Lett. **67**, 1023 (1991).
[16] D. G. Pettifor, in *Physical Metallurgy*, edited by R. W. Cahn and P. Haasen (North-Holland, Amsterdam, 1983).
[17] J. D. Jackson, *Classical Electrodynamics* (Wiley, New York, 1962).